

# Cost-effective diffuse reflectance spectroscopy device for quantifying tissue absorption and scattering *in vivo*

Bing Yu,<sup>a,\*</sup> Justin Y. Lo,<sup>a</sup> Thomas F. Kuech,<sup>b</sup> Gregory M. Palmer,<sup>c</sup> Janelle E. Bender,<sup>a</sup> and Nirmala Ramanujam<sup>a</sup>

<sup>a</sup>Duke University, Department of Biomedical Engineering, Durham, North Carolina 27708

<sup>b</sup>University of Wisconsin, Department of Chemical and Biological Engineering, Madison, Wisconsin 53706

<sup>c</sup>Duke University, Department of Radiation Oncology, Durham, North Carolina 27708

**Abstract.** A hybrid optical device that uses a multimode fiber coupled to a tunable light source for illumination and a 2.4-mm photodiode for detection in contact with the tissue surface is developed as a first step toward our goal of developing a cost-effective, miniature spectral imaging device to map tissue optical properties *in vivo*. This device coupled with an inverse Monte Carlo model of reflectance is demonstrated to accurately quantify tissue absorption and scattering in tissue-like turbid synthetic phantoms with a wide range of optical properties. The overall errors for quantifying the absorption and scattering coefficients are  $6.0 \pm 5.6$  and  $6.1 \pm 4.7\%$ , respectively. Compared with fiber-based detection, having the detector right at the tissue surface can significantly improve light collection efficiency, thus reducing the requirement for sophisticated detectors with high sensitivity, and this design can be easily expanded into a quantitative spectral imaging system for mapping tissue optical properties *in vivo*. © 2008 Society of Photo-Optical Instrumentation Engineers. [DOI: 10.1117/1.3041500]

Keywords: diffuse reflectance spectroscopy; spectral imaging.

Paper 08238LR received Jul. 15, 2008; revised manuscript received Sep. 24, 2008; accepted for publication Oct. 17, 2008; published online Dec. 15, 2008.

UV-visible diffuse reflectance spectroscopy (UV-VIS DRS) is sensitive to the absorption and scattering properties of biological molecules in tissue and thus can be used as a tool for quantitative tissue physiology *in vivo*. One major absorber of light in mucosal tissue in the visible range is hemoglobin (Hb), which shows distinctive, wavelength-dependent absorbance characteristics depending on its concentration and oxygenation. Tissue scattering is sensitive to the size and density of cellular structures such as nuclei and mitochondria. Thus, DRS of tissues can quantify changes in oxygenation, blood volume and alterations in cellular density and morphology. Some potential clinical applications of UV-VIS DRS include monitoring of tissue oxygenation,<sup>1</sup> precancer and cancer

detection,<sup>2,3</sup> intraoperative tumor margin assessment,<sup>4</sup> and assessing tumor response to cancer therapy.<sup>1</sup>

Our group has developed a fiber optic DRS system<sup>5</sup> and a fast inverse Monte Carlo (MC) model of reflectance<sup>6</sup> to non-destructively and rapidly quantify tissue absorption and scattering properties. The system consists of a 450-W xenon lamp, a monochromator, a fiber optic probe, an imaging spectrograph, and a CCD camera. Previously published studies by our group<sup>7</sup> show that this technology is capable of quantifying breast tissue physiological and morphological properties, and that these quantities can be used to discern between malignant and non-malignant tissues with sensitivities and specificities exceeding 80%. Although this technology coupled with the MC model is a robust toolbox for quantifying tissue optical properties, this system suffers from several drawbacks similar to other spectrometers. First, optical fibers when used for detection, collect a relatively small portion of the remitted signal, thus high-quantum-efficiency, low-noise detectors are required to detect the signal, particularly in the UV-blue spectral region. Optical-fiber-based detection, while reasonable for single-point sampling, is unwieldy and expensive when expanded for use in imaging applications. Thus, a simpler, low-cost, and more portable reflectance spectrometer, capable of making fast measurements and easily extendable into a spectral imaging platform for mapping tissue optical properties is desirable for clinical applications. Previous studies have attempted to develop a portable DRS probe for cancer detection. Cerussi et al.<sup>8</sup> developed a handheld ( $5 \times 8 \times 10$  cm) laser breast scanner (LBS) based on frequency-domain near-infrared spectroscopy for breast cancer detection. The LBS probe consists of a fiber bundle for illumination and an avalanche photodiode module placed 22 mm from the fiber bundle for detection. Feather et al.<sup>9</sup> reported a portable diffuse reflectometer that uses nine LEDs at three visible wavelengths to illuminate skin and a photodiode to collect diffusely reflected light, through a 7-mm aperture. The LBS has a sensing depth over 1 cm, but is difficult to multiplex into a spectral imaging device because of the size of the device. The LED-photodiode-based reflectometer is extendable to imaging, but measurements based on this device does not provide quantitative endpoints such as absorption and scattering, which relate to the underlying biology of the tissue.

Our long-term goal is to develop a cost-effective, miniature spectral imaging device for quantifying tumor physiology and morphology with performance comparable to its benchtop counterpart. In this letter, we describe a single-point hybrid optical probe that consists of a multimode illumination fiber and a silicon photodiode as a first step toward the long-term goal. We demonstrate that diffuse reflectance (DR) spectra measured with the hybrid system coupled with our inverse MC model provides quantitative measures of tissue absorption and scattering with accuracy that is comparable to that of the original benchtop system.

The hybrid system, shown in Fig. 1(a), consists of a 450-W xenon lamp and monochromator (JY Horiba, Edison, New Jersey), a 1-mm illumination optical fiber [numerical aperture (NA)=0.22], a 2.4-mm silicon photodiode (S1226, Hamamatsu, Japan) with a low-noise current amplifier (PDA-750, Terahertz Technologies Inc., Oriskany, New York), and a

\*Address all correspondence to: Bing Yu, Dept. Biomedical Engineering, Duke University, 136 Hudson Hall, Box 90281, Durham, NC 27708-0281. Tel: 919-660-5033; E-mail: bing.yu@duke.edu

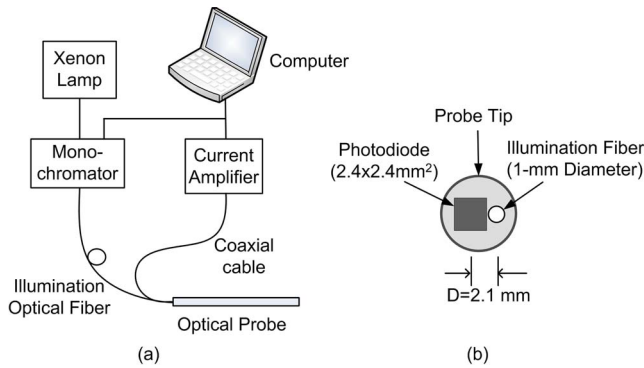


Fig. 1 Schematic of (a) modified spectrometer and (b) probe tip.

laptop computer. The hybrid system uses the same light source and monochromator and an illumination fiber with similar diameter and NA as the original system. The primary difference between the two systems is that the photodiode and current amplifier in the new system replace the collection fibers, spectrograph, and CCD camera in the original system. At the distal end of the probe [Fig. 1(b)] the edge of the photodiode was trimmed to the active area and transparent epoxy was used to bond the cleaved fiber adjacent to the photodiode, such that the center-to-center distance between the fiber and the photodiode is 2.1 mm. The overall diameter of the probe tip is 6 mm. The maximum power out of the illumination fiber was  $130 \mu\text{W}$  at 470 nm, and the minimum power was  $65 \mu\text{W}$  at 590 nm. This system has significantly lower cost and better collection efficiency than the original system because of the larger NA of the silicon photodiode (NA=0.96) and its direct contact with the sample. It can also be easily multiplexed into a spectral imaging device by interfacing a bundle of optical fibers to the exit slit of the monochromator and separating the fibers at the distal end, such that each fiber is coupled to a discrete photodiode within a large matrix of photodiodes.

To evaluate the performance of the modified system, a series of experiments were conducted on homogeneous tissue phantoms. Prior to the phantom experiments, the long-term drift and signal-to-noise ratio (SNR) of the system were characterized. We determined that the drift of the system was less than 1 nA over 2 h with the lamp on and the probe tip in contact with the surface of a liquid phantom. By taking three consecutive DR spectra from 400 to 600 nm in the darkest phantom among the 10 phantoms described in the following, we calculated an average SNR  $[=20 \log(\text{mean intensity}/\text{standard deviation})]$  of 42.9 dB over all wavelengths and a minimum SNR of 24.6 dB at 410 nm, which is close to the Soret band of oxy-Hb.

Phantoms with absorption coefficient ( $\mu_a$ ) and reduced scattering coefficient ( $\mu'_s$ ) representative of human breast tissues in the 400 to 600-nm wavelength range<sup>6</sup> were created with the scatterer, 1- $\mu\text{m}$ -diam polystyrene spheres (07310-15, Polysciences, Inc., Warrington, Pennsylvania) and variable concentrations of the absorber, Hb (H0267, Sigma Co., St. Louis, Missouri). Two sets of liquid phantoms were created by titrating the absorber at two scattering levels, and all DR measurements were made the day the phantoms were prepared. The first set of phantoms (1A to 1E) consisted of five

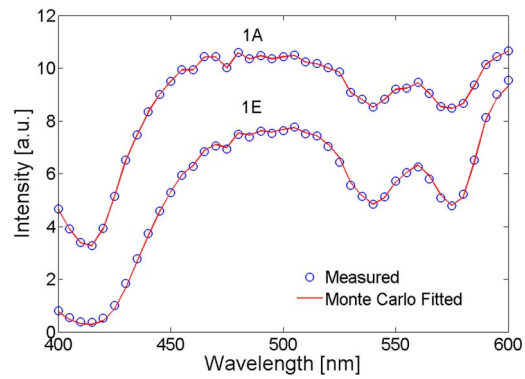


Fig. 2 Calibrated measured and MC-fitted tissue phantom spectra.

low-scattering phantoms (wavelength-averaged  $\mu'_s \approx 10.6 \text{ cm}^{-1}$ ) with wavelength-averaged  $\mu_a$  of 0.49, 0.88, 1.28, 1.58, and  $1.97 \text{ cm}^{-1}$  over the 400 to 600-nm range. The second set (2A to 2E) consisted of five high-scattering phantoms (wavelength-averaged  $\mu'_s \approx 18.5 \text{ cm}^{-1}$ ) with the same  $\mu_a$  values as the first set. A complete DR spectrum was collected from each phantom by scanning the bandpass of the monochromator (4.5 nm) from 400 to 600 nm at increments of 5 nm. Then, a DR spectrum was also obtained from a Spectralon 99% diffuse reflectance puck (SRS-99-010, Labsphere, Inc., North Sutton, New Hampshire) with the probe in contact with the puck immediately after the phantom measurements with the same instrument settings.

An inverse MC model<sup>6</sup> was used to extract the  $\mu_a$  and  $\mu'_s$  of the liquid phantoms. The model was validated in both phantom<sup>6,10</sup> and clinical studies.<sup>7</sup> The MC forward model assumes a set of absorbers (oxy-Hb with known extinction coefficients measured using a spectrophotometer in this case) are present in the medium. The scatterer (polystyrene microsphere in this study) is assumed to be single-sized, spherically shaped, and uniformly distributed. The  $\mu_a(\lambda)$  of the medium are calculated from the concentration of each absorber and the corresponding extinction coefficients using Beer's law. The  $\mu'_s(\lambda)$  and anisotropy factor are calculated using Mie theory.<sup>11</sup> The  $\mu_a(\lambda)$  and  $\mu'_s(\lambda)$  are then input into a scalable MC model of light transport to obtain a modeled DRs spectrum. In the inverse model, the modeled DR is adaptively fitted to the measured tissue DR. When the sum of square error between the modeled and measured DR is minimized, the concentrations of absorber, from which  $\mu_a$  can be derived, and  $\mu'_s$  are extracted. To experimentally compare measured phantom spectra to MC simulated phantom spectra for the fitting process, the "calibrated" DR spectrum of the target phantom for which the optical properties are to be quantified, was divided point by point by the "calibrated" DR spectrum of a reference phantom with known optical properties. The term "calibrated" in both cases refers to the normalization of the DR spectrum to that measured from the Spectralon puck for correction of the wavelength-dependent response of the instrument. In this phantom study, phantom 1C (wavelength-averaged  $\mu_a = 1.28 \text{ cm}^{-1}$ , wavelength-averaged  $\mu'_s = 10.6 \text{ cm}^{-1}$ ) was selected as a reference phantom and the remaining nine phantoms were used as targets. Bender et al. previously provided guidelines for the selection of a reference phantom.<sup>10</sup>

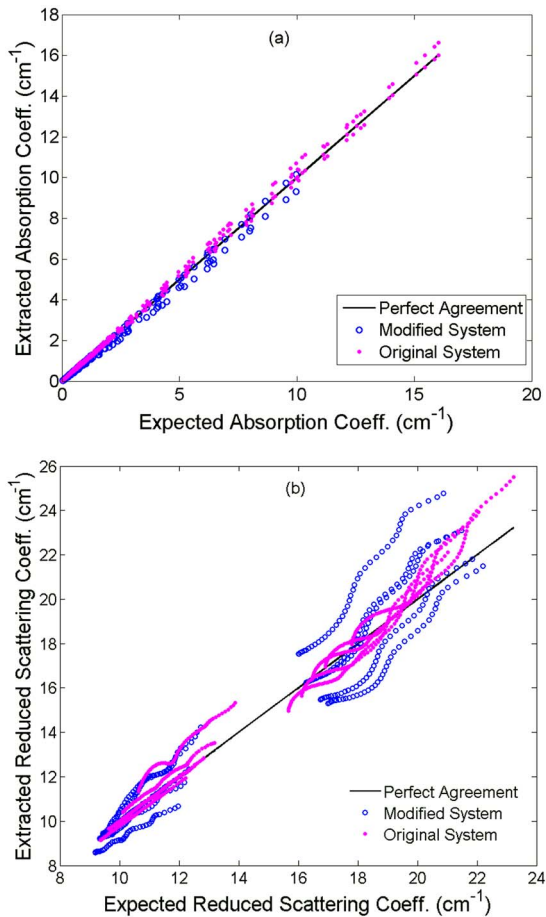


Fig. 3 Extracted versus expected (a) absorption coefficient and (b) reduced scattering coefficient.

Figure 2 shows the Spectralon puck-calibrated reflectance spectra for two phantoms 1A and 1E and the corresponding fits to the MC model. The three valleys at 415, 540, and 575 nm on the spectra for both phantoms are the Soret band (400 to 450 nm),  $\alpha$  band (540 nm), and  $\beta$  band (569 nm) of oxygenated Hb, respectively. There is excellent agreement between the measured spectra and the fits. Figures 3(a) and 3(b) show the extracted versus expected  $\mu_a$  and  $\mu'_s$  for all wavelengths over the 400 to 600-nm range quantified with the modified and original systems for the similar range of optical properties. The 10 phantoms tested with the modified system have an overall  $\mu_a$  range of 0.035 to 10  $\text{cm}^{-1}$  and a  $\mu'_s$  range of 9.2 to 22.2  $\text{cm}^{-1}$ , while that tested with the original system have overall  $\mu_a$  and  $\mu'_s$  ranges of 0.008 to 16.0  $\text{cm}^{-1}$  and 9.3 to 23.2  $\text{cm}^{-1}$ , respectively. The reference phantom used for measurements made with the original system had a wavelength-averaged  $\mu_a=2.0 \text{ cm}^{-1}$  and  $\mu'_s=10.6 \text{ cm}^{-1}$ . The correlation coefficients for  $\mu_a$  and  $\mu'_s$  are 0.9981 and 0.9588, respectively, for optical properties quantified with the modified system. An overall error of  $6.0 \pm 5.6\%$  was calculated for  $\mu_a$  and  $6.1 \pm 4.7\%$  for  $\mu'_s$  for the modified system. For the purposes of comparison, the original system had a overall errors  $5.8 \pm 5.1$  and  $3.0 \pm 3.1\%$  for extracting  $\mu_a$  and  $\mu'_s$ , respectively.

The modified system can quantify absorption from phantoms with modest absorption coefficients (up to 10  $\text{cm}^{-1}$ ). Compared to the original system, the modified system has higher errors in extraction of scattering coefficient due to its 10 to 15-dB lower SNR for high scattering. The dynamic range of the system may be improved by decreasing the center-to-center distance between the source and detector as well as by increasing the area of the photodiode.

We believe that the modified system combined with our MC model can be extended into an optical spectral imaging system to map out the concentrations of absorbers and the bulk tissue scattering properties of subsurface tissue volumes, which are on a length scale of several millimeters. There are a number of applications for which this technology would be ideally suited, including epithelial precancer and cancer detection (such as those of the skin, oral cavity, and cervix), intra-operative tumor margin assessment, and the monitoring of tumor response to therapy in organ sites such as the head and neck and cervix. More importantly, placing the detector directly at the tissue surface will improve collection efficiency and will significantly reduce the cost associated with expensive and sophisticated CCDs.

Acknowledgments

This work has been funded by a Department of Defense Breast Cancer Research Program (DOD BRCP) Era of Hope Scholar award to Dr. Nirmala Ramanujam.

References

1. I. J. Bigio and S. G. Bown, "Spectroscopic sensing of cancer and cancer therapy, current status of translational research," *Cancer Biother* **3**(3), 259–267 (2004).
2. G. Zonios, L. T. Perelman, V. Backman, R. Manoharan, M. Fitzmaurice, J. Van Dam, and M. S. Feld, "Diffuse reflectance spectroscopy of human adenomatous colon polyps *in vivo*," *Appl. Opt.* **38**(31), 6628–6637 (1999).
3. Y. N. Mirabal, S. K. Chang, E. N. Atkinson, A. Malpica, M. Follen, and R. Richards-Kortum, "Reflectance spectroscopy for *in vivo* detection of cervical precancer," *J. Biomed. Opt.* **7**(4), 587–594 (2002).
4. W. C. Lin, S. A. Toms, M. Johnson, E. D. Jansen, and A. Mahadevan-Jansen, "In vivo brain tumor demarcation using optical spectroscopy," *Photochem. Photobiol.* **73**(4), 396–402 (2001).
5. C. Zhu, G. M. Palmer, T. M. Breslin, F. Xu, and N. Ramanujam, "Use of a multiseparation fiber optic probe for the optical diagnosis of breast cancer," *J. Biomed. Opt.* **10**(2), 024032 (2005).
6. G. M. Palmer and N. Ramanujam, "Monte Carlo-based inverse model for calculating tissue optical properties. Part I, Theory and validation on synthetic phantoms," *Appl. Opt.* **45**(5), 1062–1071 (2006).
7. C. Zhu, G. M. Palmer, T. M. Breslin, J. Harter, and N. Ramanujam, "Diagnosis of breast cancer using diffuse reflectance spectroscopy: comparison of a Monte Carlo versus partial least squares analysis based feature extraction technique," *Lasers Surg. Med.* **38**(7), 714–724 (2006).
8. A. Cerussi, N. Shah, D. Hsiang, A. Durkin, J. Butler, and B. J. Tromberg, "In vivo absorption, scattering, and physiologic properties of 58 malignant breast tumors determined by broadband diffuse optical spectroscopy," *J. Biomed. Opt.* **11**(4), 044005 (2006).
9. J. W. Feather, D. J. Ellis, and G. Leslie, "A portable reflectometer for the rapid quantification of cutaneous haemoglobin and melanin," *Phys. Med. Biol.* **33**(6), 711–722 (1988).
10. J. E. Bender, K. Vishwanath, L. K. Moore, J. Q. Brown, V. Chang, G. M. Palmer, and N. Ramanujam, "A robust Monte Carlo model for the extraction of biological absorption and scattering *in vivo*," *IEEE Trans. Biomed. Eng.* (in press).
11. B. C. F. Huffman, *Absorption and Scattering of Light by Small Particles*, Wiley, New York (1998).